

# **Improving early warning of drought-driven food insecurity in Southern Africa using operational hydrological monitoring and forecasting products**

Shraddhanand Shukla<sup>1</sup>, Kristi R. Arsenault<sup>2,3</sup>, Abheera Hazra<sup>4,3</sup>, Christa Peters-Lidard<sup>3</sup>, Randal D. Koster<sup>3</sup>, Frank Davenport<sup>1</sup>, Tamuka Magadzire<sup>5,1</sup>, Chris Funk<sup>6,1</sup>, Sujay Kumar<sup>3</sup>, Amy McNally<sup>2,5</sup>, Augusto Getirana<sup>4,3</sup>, Greg Husak<sup>1</sup>, Ben Zaitchik<sup>7</sup>, Jim Verdin<sup>8,5</sup>, Faka Dieudonne Nsadisa<sup>9</sup>, Inbal Becker-Reshef<sup>3,4</sup>

<sup>1</sup>University of California, Santa Barbara, California, USA

<sup>2</sup>SAIC, Reston, Virginia, USA

<sup>3</sup>NASA Goddard Space Flight Center, Greenbelt, Maryland, USA

<sup>4</sup>University of Maryland, Maryland, USA

<sup>5</sup>Famine Early Warning Systems Network, Washington D.C., USA

<sup>6</sup>EROS, United States Geological Survey, Sioux Falls, South Dakota, USA

<sup>7</sup>John Hopkins University, Baltimore, Maryland, USA

<sup>8</sup>United States Agency for International Development, Washington D.C., USA

<sup>9</sup>Southern African Development Community Climate Services Center, Botswana

*Correspondence to:* Shraddhanand Shukla ([sshukla@ucsb.edu](mailto:sshukla@ucsb.edu))

## **Abstract:**

1 The region of southern Africa (SA) has a fragile food economy and is vulnerable to frequent  
2 droughts. Interventions to mitigate food insecurity impacts require early warning of droughts —  
3 preferably as early as possible before the harvest season (typically, starting in April) and lean  
4 season (typically, starting in November). Hydrologic monitoring and forecasting systems provide  
5 a unique opportunity to support early warning efforts, since they can provide regular updates on  
6 available rootzone soil moisture (RZSM), a critical variable for crop yield, and provide forecasts  
7 of RZSM by combining the estimates of antecedent soil moisture conditions with climate  
8 forecasts. For SA, this study documents the predictive capabilities of RZSM products from a  
9 recently developed NASA Hydrological Forecasting and Analysis System (NHyFAS). Results  
10 show that the NHyFAS products would have identified the regional severe drought event—  
11 which peaked during December-February of 2015/2016—at least as early as November 1, 2015.  
12 Next, it is shown that during 1982-2016, February RZSM forecasts [monitoring product]  
13 available in early November [early March] have a correlation of 0.49 [0.79] with the detrended  
14 regional crop yield. It is also found that when the February RZSM forecast [monitoring product]  
15 available in early November [early March] is indicated to be in the lowest tercile, the detrended  
16 regional crop yield is below normal about two-thirds of the time [always], at least over the  
17 sample years considered. Additionally, it is shown that February RZSM forecast [monitoring  
18 product] can provide “out-of-sample” crop yield forecasts with comparable [substantially better  
19 with 40% reduction in mean error] skill to December-February ENSO. These results indicate that  
20 the NHyFAS products can effectively support food insecurity early warning in the SA region.  
21 Finally, since a framework similar to NHyFAS can be used to provide RZSM monitoring and

- 22 forecasting products over other regions of the globe, this case study also demonstrates potential
- 23 for supporting food insecurity early warning globally.

## 24 **1 Introduction**

25 Southern Africa (SA) is vulnerable to food insecurity. Droughts driven by climate stressors (e.g.  
26 precipitation and temperature) are among the important drivers of food insecurity (Misselhorn  
27 2005; Conway et al. 2015). Moreover, anthropogenic climate change is shown to increase the  
28 likelihood of climate-driven flash droughts (Yuan et al., 2018). The primary rainy season in SA  
29 spans from October to March, which overlaps the main planting season from October to  
30 February (Fig. 1 [a]). This period also covers the lean season, when food supplies from the prior  
31 year's harvest become limited. April-July is typically the main harvest season, when the food  
32 reserve is expected to begin replenishing. In several SA countries, with the Republic of South  
33 Africa (RSA) being the main exception, typical monthly variability in food prices closely follows  
34 this crop cycle, as shown in Fig. 1(b). The prices typically start to rise after the harvest season  
35 and reach their peak just before or near the start of the harvest season. This correspondence  
36 between the prices and crop cycles highlights the region's climate-related sensitivity to food  
37 insecurity. In the case of below-normal crop yield, the food prices rise even more than normal,  
38 reducing access to food for the poorest of the population.

39 The percentage income shared by the poorest 10% and 20% of the population in several  
40 SA countries has not improved significantly over time (not shown here). These portions of the  
41 population are likely to be more food insecure in drought years; they already use a relatively  
42 higher share of their income on food, and in the case of price rises related to low crop yield, their  
43 access to food becomes even more limited.

44 The 2015-16 drought event (attributed to a strong El Niño) in SA further highlighted its  
45 vulnerability to climate-related regional food insecurity (Archer et al., 2017; Funk et al., 2018;  
46 Pomposi et al., 2018). This event led to a substantial reduction in regional agricultural production

47 —including in the RSA, which is the main crop-producing country in the region—a reduction  
48 and rationing of water supplies, a loss of livestock, and an increase in unemployment in the  
49 region, and it pushed 29 million people into severe food insecurity (SADC, 2016). Throughout  
50 the Southern African Development Community (SADC) region in 2015-16, cereal production  
51 was down by -10.2% (varying from +61% to -94% in individual member countries) relative to  
52 the previous 5-year average (SADC, 2016). Figure 1 (c)-(f) shows a comparison of national retail  
53 maize prices (in USD) in several of the SA countries during 2015-16, with the previous 5-year  
54 mean prices in those countries. The prices in 2015-16 were substantially higher than the previous  
55 5-year mean. Of particular importance is the price increase in RSA, where, typically, the food  
56 prices do not vary much throughout the year due to its general self-sufficiency in food  
57 production, as well as its international trade. Consumer Price Index (CPI) for food for the RSA  
58 also experienced a drastic upward shift during the 2015-16 drought year (not shown here). In  
59 fact, based on the CPI data (available from the FAO), the CPI was substantially higher than that  
60 of the past 5-year mean during the beginning of the following growing season of 2016-17,  
61 including in the RSA where typically the CPI remains fairly stable during a year. These price  
62 shocks can dramatically impact poor households, which typically spend 60% or more of their  
63 income on food. According to the recent World Development Indicator ([World Bank 2016](#)),  
64 incomes for the poorest 10% and 20% of households in these countries have remained generally  
65 constant, underscoring the depth of poverty (Figure 2). On average, in Malawi, Mozambique,  
66 Zimbabwe, and South Africa, these individuals subsist on USD 70, 126, 288, and 716 a year,  
67 respectively.

68 Figure 1(c)-(f) and the income-related facts (based on World Bank Development  
69 Indicator) presented above highlight the severity of food insecurity in a regional drought event

70 like 2015-16. In the 2015-2016 event, food imports from the RSA—which is the main producer  
71 and exporter of food in the region to the other SA countries—were not enough, and international  
72 assistance became crucial. This is why in June 2016, the SADC launched a Regional  
73 Humanitarian Appeal stating that approximately 40 million people in the region required  
74 humanitarian assistance, at a cost of approximately USD 2.4 billion (Magadzire et al. 2017).

75 Mitigation of the most adverse impacts of food insecurity, like the event of 2015-16,  
76 requires timely and effective early warning. An effective early warning system has two key  
77 attributes (Funk et al., 2019): (1) the ability to provide routine, frequent early warning of drought  
78 status and (2) the ability to incorporate both monitoring and forecasting to best account for the  
79 conditions up to the date of early warning, in combination with the climate outlook for the  
80 upcoming season.

81 A seasonal-scale hydrologic forecasting system can potentially support an early warning  
82 system, as it can provide updated hydrologic forecasts on a monthly basis by accounting for the  
83 drought conditions as of the forecast release date and climate outlook over the forecast period  
84 (Sheffield et al., 2014; Shukla et al., 2014; Yuan et al., 2013). However, thus far, the application  
85 of seasonal-scale hydrologic forecasts in food insecurity early warning has been limited at best,  
86 with the only other main example being the African Flood and Drought Monitor (Sheffield et al.,  
87 2014).

88 On the other hand, operational, publicly available, state-of-the-art dynamical climate  
89 forecasts have found regular usage in guiding climate outlooks, as well as assessments of  
90 expected food insecurity. For example, USAID’s Famine Early Warning Systems Network  
91 (<http://fews.net/>), G20-Group on Earth Observations Global Agricultural Monitoring  
92 (GEOGLAM) Crop Monitor for Early Warning, and SADC’s Climate Service Center (CSC) all

93 utilize the dynamical climate forecasts as one of their early warning tools. Furthermore,  
94 numerous past studies have investigated the predictability of SA climate (Meque and Abiodun,  
95 2014) and examined the skill of diverse approaches in forecasting, particularly of rainfall, as well  
96 as streamflow and agricultural production in different parts of this region (Archer et al., 2017;  
97 Cane et al., 1994; Diro, 2015; Landman et al., 2001; Landman and Beraki, 2010; Landman and  
98 Goddard, 2002; Manatsa et al., 2015; Martin et al., 2000; Sunday et al., 2014; Trambauer et al.,  
99 2015; Winsemius et al., 2014). Historically, El Niño-Southern Oscillation (ENSO) has proven to  
100 be among the main predictors of this region's climate, with another important predictor being the  
101 Southern Indian Ocean Dipole (Hoell et al., 2016, 2017; Hoell and Cheng, 2017).

102 In August 2018, a new NASA Hydrological Forecasting and Analysis System  
103 (NHyFAS), an operational seasonal hydrologic forecasting system (Arsenault et al., 2020), was  
104 implemented to support the early warning efforts of FEWS NET, building upon existing  
105 hydrologic monitoring (McNally et al., 2017). This study evaluates this system's ability to  
106 support early warning of regional food insecurity in the SA region. The evaluation is conducted  
107 by examining the performance of this system (i) for the 2015-16 drought event, which led to  
108 regional food insecurity, (ii) in explaining regional crop yield variability in the region, and (iii) in  
109 identifying below-normal crop yield events, which are characteristically associated with overall  
110 lower food availability in the region and, hence, food insecurity. Regional crop yield is used as a  
111 target variable here, as it is among the main contributors to regional food insecurity. It is  
112 hypothesized that if this system can skillfully forecast regional crop yield and identify below-  
113 normal regional crop yields, it can successfully support the early warning of food insecurity in  
114 the region.

115 As noted above and shown in Fig. 1(a), April-July is typically the main harvest season,  
116 when the food reserve is expected to begin replenishing and last through the lean season, which  
117 starts in November. Below-normal food availability during this period can lead to food  
118 insecurity. Therefore, early warning systems aim to provide outlooks for food insecurity as far in  
119 advance of the harvest and lean season as possible. Consequently, this study focuses on using  
120 forecasting and monitoring products that are available in November (4-5 months before the start  
121 of the harvest, and about a year before the start of the next lean season) through March (1-2  
122 months before the start of the harvest, and about 8-9 months before the start of the next lean  
123 season) to examine their value in supporting early warning of food insecurity in the region.

## 124 **2 Data and Methodology**

125 The hydrologic monitoring and forecasting products used in this study come from the  
126 NHyFAS (Fig. 3) (Arsenault et al., 2020). Figure 3 shows an overview of the implementation of  
127 the NHyFAS for the purpose of this study. Because Arsenault et al. (2020) already describes the  
128 system in detail, we simply provide here a brief description of the hydrologic models (section  
129 2.1), the model parameters (section 2.2), the input observed forcings and climate forecasts  
130 (section 2.3), and the RZSM monitoring and forecasting products (section 2.4) used in the  
131 present study. The reported crop yield data used in this study are described in section 2.5.

### 132 **2.1 Hydrologic Modeling Framework**

133 To generate hydrological forecasts, we use NASA's Catchment land surface model  
134 (CLSM; (Ducharne et al., 2000; Koster et al., 2000) and the Noah Multi-Parameterization (Noah-  
135 MP; (Niu et al., 2011; Yang et al., 2011) land surface model (LSM), which compute changes in  
136 soil moisture (e.g., root zone) and groundwater storage in response to computed surface energy  
137 and water fluxes. These two LSMs are part of the model suite in the Land Information System



138 (LIS) framework (Kumar et al., 2006)—the primary software system used to produce this study’s  
139 forecast experiments. Both LSMs were spun-up using two cycles of forcing for the period from 1  
140 January, 1981 to 31 December, 2015; then, historical open-loop (OL) runs were generated for  
141 January 1981 through 2018. Rootzone SM (RZSM), which is the main hydrologic variable used  
142 in this analysis, represents the soil moisture in the top one meter of the soil profile. The entire  
143 depth of the soil profile is different for the two models used in this analysis (typically about 2 m  
144 for Noah-MP, and about 4 m for CLSM).

## 145 **2.2 Model Parameters**

146 In the version of CLSM used here, hydrologic and catchment parameters (Ducharne et  
147 al., 2000) are based on a high-resolution, global topographic data set (Verdin and Verdin, 1999),  
148 and soil texture (Reynolds et al., 2000) and profile parameters are derived from the Second  
149 Global Soil Wetness Project (GSWP-2; Guo and Dirmeyer, 2006) data set and mapped to the  
150 catchment tiles. Land cover classes are mapped from the University of Maryland AVHRR data  
151 set, and vegetation parameters include, for example, leaf area index (LAI), which is also derived  
152 from GSWP-2. Albedo scaling factors are based on Moderate Resolution Imaging  
153 Spectroradiometer (MODIS) direct and diffuse visible or near infra-red radiation inputs (Moody  
154 et al., 2008).

155 Noah-MP vegetation parameters include the modified IGBP MODIS-based land cover  
156 data set (Friedl et al., 2002), leaf area index, and monthly greenness fraction (Gutman and  
157 Ignatov, 1998). The soil texture data set is based on Reynolds et al. (2000), and soil parameters  
158 are mapped to the varying textures. Monthly global (snow-free) albedo (Csiszar and Gutman,  
159 1999) and a maximum snow albedo parameter field are also employed. Additional details are  
160 found in (Niu et al., 2011).

### 161 **2.3 Input observed forcings and climate forecasts**

162 The spin-up and OL runs used to generate the long-term “observed” climatology of  
163 RZSM are driven with NASA’s Modern-Era Retrospective analysis for Research and  
164 Applications, version 2 (MERRA-2; [Gelaro et al., 2017]) atmospheric fields (e.g., 2m air  
165 temperature, humidity). Precipitation forcing comes from the U.S. Geological Survey  
166 (USGS)/University of California, Santa Barbara (UCSB) Climate Hazards Center InfraRed  
167 Precipitation with Station data set, version 2.0 (CHIRPSv2; [Funk et al., 2015]).

168 Hindcasts of RZSM are generated by forcing the hydrologic models with NASA’s  
169 Goddard Earth Observing System (GEOS) Atmosphere-Ocean General Circulation Model,  
170 version 5 (GEOS; [Borovikov et al., 2017]) Seasonal-to-Interannual Forecast System. The eleven  
171 ensemble members of version 1 of this forecast system that were used in the North American  
172 Multi-Model Ensemble (NMME) project are used in the forecast portion of this study. To make  
173 the GEOS forecasted meteorology consistent with the meteorology underlying the OL initial  
174 conditions, we Bias-Corrected and Spatially Downscaled (BCSD; [Wood et al., 2002]) the  
175 GEOS forecasts using the MERRA-2 and CHIRPS data sets. The BCSD-GEOS forecast files are  
176 then ingested into LIS to drive the LSMs and generate the dynamical hydrological forecasts. The  
177 BCSD-GEOS hindcasts are initialized on November 1st (near the start of the planting season)  
178 and January 1st (middle of the planting season) of each year in 1982-83 to 2017-18. Each  
179 hindcast is run for 6 months.

180 Hindcasts of RZSM are also generated using the Ensemble Streamflow Prediction (ESP)  
181 method (Day 1985; Shukla et al. 2013), where the models are forced with resampled observed  
182 forcings (forcings that are used to drive the OL simulation) taken from 1982-2010 period. The

183 hindcasts generated using the ESP method derive their skills from the initial hydrologic  
184 conditions only.

#### 185 **2.4 RZSM Monitoring and forecasting products**

186 The performance of the NHyFAS system is evaluated mainly through its RZSM  
187 monitoring (generated from OL) and forecasting products. RZSM indicates the soil moisture in  
188 the top one meter of the soil profile. Typically, the length of the roots of crops such as maize  
189 (main crop in the region of SA) is close to one meter, hence the choice of RZSM as the key  
190 forecast variable. Moreover, the entire depth of the soil profile is different for the two models  
191 used in this analysis, typically about 2 m for Noah-MP and about 4 m for CLSM; hence RZSM  
192 also allows for a consistent way to merge soil moisture products from both models.

193 Both products are generated at 0.25 X 0.25 degree spatial resolution and daily temporal  
194 resolution. Daily values are averaged over a month to get monthly values. The monthly values of  
195 the monitoring product are converted to percentiles relative to OL climatology over 1982-2010,  
196 and monthly values of the ensemble mean forecasting products (GEOS and ESP based) are  
197 converted into percentiles relative to the (ensemble mean) climatology over 1982-2010 of the  
198 respective hindcast runs. In both cases, empirical distribution is considered to convert values to  
199 percentiles. Once gridded percentile values are generated, they are spatially aggregated over the  
200 SA region (as shown in Fig. 2) to get RZSM monitoring and forecasting products over the SA  
201 region.

#### 202 **2.5 Regional Crop Yield**

203 The regional crop yield is calculated using country-level crop production and area  
204 harvested reports. These reports come from the United States Department of Agriculture's  
205 Foreign Agricultural Service's Production Supply and Distribution (PSD) database. To compile

206 this database, USDA relies on several sources, including official country statistics, reports from  
207 agricultural attaches at U.S. embassies, data from international organizations, publications from  
208 individual countries, and information from traders both inside and outside of the target countries.  
209 For this study, we focus only on maize, as it is the main crop in the region and the key crop for  
210 food security. To get regional crop yield from country-level crop yield, we first converted  
211 country-level yield into production using the harvested area (provided by the PSD), added the  
212 total production, and then divided it by the sum of the harvested area in all SA countries in our  
213 focus domain. The regional crop yield is detrended for the purposes of this study to reduce the  
214 effect of any long-term changes (e.g. technological changes) on the crop yield.

215

## 216 **2.6 Out-of-sample crop yield forecasting**

217 We also evaluate the NHyFAS RZSM monitoring and forecasting products' performance  
218 in supporting food insecurity early warning in SA through a series of out-of-sample crop  
219 forecasting experiments. Specifically, we compare the accuracy of crop yield forecasts made  
220 with NHyFAS products against univariate yield forecasts (using only the past yields) and yield  
221 forecasts made with ENSO, a widely used predictor for crop yield in this region. This evaluation  
222 has a direct implication on the usage of NHyFAS products for operational purposes, as crop yield  
223 forecasts are a common tool in food security analysis and response (Davenport et al., 2019).

224 Our baseline model is a univariate (no exogenous predictors) Autoregressive Integrated  
225 Moving Average (ARIMA) model,

$$226 \quad y'_t = \phi_1 y'_{t-1} + \dots + \phi_p y'_{t-p} + \theta_1 \varepsilon_{t-1} + \dots + \theta_q \varepsilon_{t-q} + \varepsilon_t, \quad (1)$$

227 Where  $y'_t$  is the time series of observed yields (and the ` indicates potential differencing of the  
228 time series),  $p$  is the order of lags,  $\phi$  are the autoregressive parameters,  $q$  is the order of moving

229 averages,  $\theta$  are the moving average parameters, and  $\epsilon$  are forecast errors from the prior periods.  
230 ARIMA(p,d,q) models are standard and frequently used methods for time series analysis and  
231 forecasting (Hyndman and Athanasopoulos, 2018; Hyndman and Khandakar, 2007). As  
232 discussed above, we compare the forecast performance of univariate ARIMA models eq.[1], with  
233 ARIMA models that also include environmental exogenous predictors, which, in this case, are (i)  
234 DJF ENSO (ii) February RZSM monitoring product and (iii) February RZSM forecast initialized  
235 on Nov. 1, during the growing season preceding harvested yields in year  $t$  (e.g. 1982/83 DJF  
236 used for 1983 yield). All models are fit using the `auto.arima()` function from the forecast  
237 package in the R software language.

238 We use the period of 1983-2007 (25 years) as a training period and then provide “out-of-  
239 sample” forecasts of crop yield starting in 2008. The training period always spans through the  
240 year before the target forecast year. For example, the model fit over 1983-2008 is used to  
241 forecast yields in 2009, and the model fit over 1983-2009 is used to forecast yield in 2010, and  
242 so on. We repeat this exercise through 2018 and record the one-step-ahead prediction error in  
243 each iteration. In this way, we emulate the forecasting process that food security analysts in the  
244 region go through during every year prior to harvest.

245

### 246 **3. Results**

#### 247 **3.1 Performance of NHyFAS during the 2015-16 drought event**

248 As highlighted in section 1, the 2015-16 drought event in SA is among the most severe in  
249 terms of drought severity and food insecurity impacts in the last few decades. Therefore, we  
250 begin the evaluation of the suitability of NHyFAS in supporting food insecurity early warning in  
251 the SA region by examining how this system would have performed during the 2015-16 event.

252 Although the NHyFAS operationally provides the seasonal forecasts every month, for the  
253 purpose of this study, we focus on the forecast initialized on November 1 (near the start of the  
254 planting season) and January 1 (near the middle of the growing season) of 2015-16 event. Figure  
255 4 shows the RZSM forecasts for the growing season made on November 1, 2015. By this time in  
256 the season, both FEWS NET and SADC had provided early warning of poor rainfall  
257 performance in the region (Magadzire et al, 2017). The NHyFAS RZSM forecasts would have  
258 provided further evidence of a looming unprecedented drought in the region. These forecasts  
259 would have also indicated that RSA, which is the most important country for the region’s food  
260 production, was going to be within the epicenter of this drought event. These forecasts, in turn,  
261 could potentially have triggered earlier appropriate actions by the early warning agencies, as well  
262 as the decision-makers (e.g., national governments and international relief agencies).

263 Later in the season, as the observed precipitation data became available, RZSM  
264 monitoring products would have provided refined estimates of the spatial extent and severity of  
265 drought in the region. Figure 4 (bottom panel) shows the RZSM monitoring product available  
266 after each of the months of November 2015 through February 2016. This monitoring product  
267 would have provided additional proof of the drought occurrence in the region, and shown that  
268 RSA was within the epicenter of this drought. It is important to state that even the monitoring  
269 product can be effectively used as a predictor of food insecurity events, as they are available  
270 before the typical start of the harvest season (in April) and the lean season (in November).

### 271 **3.2 Performance of NHyFAS in supporting food insecurity early warning**

272 Next, we investigate the long-term performance of NHyFAS in supporting food  
273 insecurity early warning by examining how well forecasting and monitoring products available  
274 from this system can explain historical variability in regional crop yield of the SA region and in

275 particular, help identify below-normal regional yield events. Regional crop yield is calculated by  
276 adding the yearly productions from the SA countries, then dividing it by the yearly total  
277 harvested area. The regional crop yield is then detrended to remove the effect of any long-term  
278 changes (such as technological changes) on the regional yield.

279 First, we show in Figure 5 how detrended crop yield correlates (from early November to  
280 early March) with the monthly RZSM monitoring product relative to how it correlates with 3-  
281 monthly seasonal precipitation and air temperature. The results indicate that the monthly RZSM  
282 monitoring product generally correlates better with detrended crop yield than with the seasonal  
283 precipitation or air temperature, with the correlation reaching its peak by early March, when the  
284 Feb-RZSM monitoring product and December-February precipitation and temperature are  
285 available. Feb-RZSM still shows higher correlation than seasonal precipitation and temperature;  
286 however, the difference in correlation is not statistically significant.

287 Next, the correlation between detrended crop yield and February RZSM forecasts (based  
288 on ESP method and bias-corrected GEOS forecasts) initialized on November 1 (Fig. 6a) and  
289 January 1 (Fig. 6b) is analyzed. The correlation of the yield with GEOS-based February RZSM  
290 forecasts initialized on November 1 is 0.49, which is substantially higher than that of ESP-based  
291 RZSM forecasts (0.16), clearly demonstrating the added value of using GEOS-based climate  
292 forecasts. Similarly, the correlation of yield with the GEOS-based February RZSM forecasts  
293 initialized on January 1 is 0.45, higher than that of the ESP-based forecasts (0.30) at that time of  
294 the year. Moreover, the correlation of detrended crop yield with GEOS-based February RZSM  
295 forecasts initialized on November 1 (0.49) and January 1 (0.45) is higher than that with the  
296 RZSM monitoring product (Figure 5) at those times of the year ( $<0.1$  in early November and  
297  $<0.4$  in early January). Again, this highlights the value of using forecasts of Feb-RZSM through

298 early January in supporting food insecurity early warning. Figure 6c shows that Feb-RZSM  
299 monitoring product, which is available in early March, has the highest correlation of 0.79 with  
300 the detrended crop yield.

301 Next, we examine how well the forecasting and monitoring RZSM products do in  
302 providing early warning of below-normal crop yield events. This criterion for performance  
303 evaluation is of particular significance for food insecurity early warning in the region, as below-  
304 normal crop yield events are the ones that generally lead to food insecurity. In this case, below-  
305 normal regional crop yield events are the events that lie in the bottom 18 (i.e. bottom half) when  
306 detrended crop yields for the 36 years are ranked in ascending order.

307 We calculate the probability of below-normal crop yield events when either the February  
308 RZSM forecast (initialized on November 1 and January 1) or the RZSM monitoring product for  
309 the month of November (available in early December) through the month of February (available  
310 in early March) is in the lowest tercile. RZSM products in this tercile are those lying in the  
311 bottom 12 of the RZSM products when ranked in ascending order. In the case of RZSM, the  
312 ranked climatology is different for each of the forecasting products and the monitoring products  
313 for each month. We use the lower tercile values of RZSM monitoring and forecasting products to  
314 focus on the drought years as indicated by those products. Because SA is a mostly rainfed region,  
315 the crop yield is generally below normal during drought years, as indicated in several recent  
316 events (2014-15, 2015-16, 2018-19).

317 Figure 7 shows the fraction of years with below-normal crop yield when February RZSM  
318 forecasts (made on November 1 or January 1) were in the lower tercile (shown by blue color  
319 bars) or when monthly RZSM monitoring products (shown by green color bars) were in the  
320 lower tercile. These results indicate that as early as November 1, if the February RZSM is being



321 forecasted to be in the lower tercile, then there is about ~66% probability of the regional crop  
322 yield being below normal (statistically significant at 86% confidence level). This would be 4-5  
323 months before the start of the harvest season, and about one year before the start of the next lean  
324 season. The inferred probability value increases to ~83% when the February RZSM forecasts,  
325 initialized in January, are in the lower tercile (statistically significant >95% confidence level).  
326 Finally, by early March, when the February RZSM monitoring product is available, the inferred  
327 probability increases to 100% (statistically significant >95% confidence level). In other words,  
328 over 1982-2016, whenever the February RZSM monitoring product for the SA region was in the  
329 lowest tercile, the crop yield in the following season had been below normal (based on detrended  
330 yield). This would be 1-2 months before the start of the harvest season, and about 8-9 months  
331 before the start of the next lean season.

332         Of course, the estimation of these probabilities is necessarily limited by the small sample  
333 sizes examined; the actual probability of low crop yield based on low February RZSM, for  
334 example, while apparently high, is not a full 100%. Nevertheless, these results provide, overall,  
335 further evidence of the suitability of the forecasting and monitoring products from the NHyFAS  
336 in supporting early warning of food insecurity in the region.

337

### 338 **3.3 Performance of NHyFAS in providing routine operational crop yield forecasts**

339         Finally, we evaluate the performance of NHyFAS for supporting food insecurity early  
340 warning in SA by examining the accuracy of RZSM monitoring and RZSM forecasting products  
341 in predicting regional crop yields. We compare the crop yield forecasts made with the RSZM  
342 products against both univariate forecasts (using only past observed crop yields) and forecasts  
343 made with ENSO. As ENSO is a widely used predictor for precipitation and crop yield forecasts

344 in this region, we examine the added value of using NHyFAS RZSM monitoring and forecasting  
345 products above and beyond ENSO. All forecasts are done using ARIMA models described in  
346 section 2.6.

347 Figure 8 shows a comparison between the “observed” reported crop yield (black lines)  
348 and the “out-of-sample” (i.e. post-training period) forecasted yield (red lines) produced with a  
349 univariate model, and the models using environmental exogenous predictors (i) DJF ENSO, (ii)  
350 Feb-RZSM (monitoring) product, (iii) Feb-RZSM (Forecasting product) initialized on Nov. 1., in  
351 addition to that univariate model.

352 The results indicate that: (i) environmental predictors such as ENSO and the NHyFAS products  
353 can make crop yield forecasts that are more accurate than those produced using only a univariate  
354 approach. When ENSO is used as an additional predictor (in addition to a Univariate model), the  
355 MAE reduces from 0.342 MT/HA to 0.285 MT/HA, a ~17% reduction in error. (ii) Use of the  
356 Feb-RZSM monitoring product has an even larger impact, reducing the MAE by about 50%, to  
357 0.174 MT/HA. (iii) Use of the Feb-RZSM forecasting product (initialized on Nov 1) has an  
358 impact similar to that of DJF ENSO. Although the MAE is about 6% larger when the forecasting  
359 product is used rather than the ENSO predictor, the forecasting product has the significant  
360 advantage of being available for about 4 months earlier. For comparison (not shown here) MAE  
361 of Feb-RZSM forecasting product (initialized on Nov 1) is slightly smaller (~6%) than the MAE  
362 of August-October (ASO)-ENSO (also available in early Nov) and is comparable to the MAE of  
363 September-November (SON)-ENSO (available in early December) as a predictor of crop yield  
364 forecast.

365 Table 1 shows the number of times the observed yield is within the 80% confidence  
366 interval of the forecasts and the mean spread of the confidence interval. The improvement in

367 performance obtained when the Feb-RZSM monitoring product is used is clear; during 10 of the  
368 11 years in the validation period, the observed yield falls within the 80% confidence interval,  
369 whereas this happens in only 7 years when DJF ENSO is used as the additional predictor. The  
370 mean spread of the confidence interval associated with the use of the Feb-RZSM monitoring  
371 product (0.70 MT/HA) is also the smallest.

## 372 **4 Discussion**

373

374 This study makes a case for the application of NHyFAS's RZSM forecasting and  
375 monitoring products in supporting the early warning of food insecurity in SA. It has been shown  
376 that the successful early warning of crop yield, and especially below-normal crop yield years,  
377 can be issued based on these products. In this section, we address a few important caveats.

378

### 379 **4.1 Comparison with existing drought forecasting systems and approaches:**

380 In this study, we keep the comparison with existing forecasting systems and approaches  
381 limited to the comparison of the performance of NHyFAS products with (i) ESP (i.e.  
382 climatology) based RZSM forecasts and (ii) ENSO-based crop yield forecasts, both of which are  
383 commonly used approaches for drought forecasting in the region, including by early warning  
384 agencies such as FEWS NET. Comparison against both approaches shows clear added value of  
385 using the NHyFAS products. We could not compare the performance of the NHyFAS with  
386 FEWS NET or SADC's official historical forecasts because:

387 (i) FEWS NET's official forecast is an outlook of food insecurity conditions ([Funk et al. 2019](#))  
388 (<https://fews.net/>) which is based not only on agroclimatology (i.e., agriculture and climate  
389 conditions) but also on market conditions and nutrition and livelihood conditions. The NHyFAS  
390 forecasts that are now being used by FEWS NET would fall into the category of

391 agroclimatological conditions. In fact, the goal of the evaluation of the NHyFAS forecasts is to  
392 establish whether NHyFAS forecasts can be suitable agroclimatological forecast inputs for  
393 FEWS NET to guide the development of food insecurity outlook assessments. Also, FEWS NET  
394 Food Insecurity Outlook is partly based on subjective assessments, in some ways similar to the  
395 U.S. drought monitor (Svoboda et al., 2002) or U.S. Seasonal Drought Outlook, in addition to  
396 quantitative assessments such as agroclimatological forecasts. Finally, FEWS NET's archive of  
397 Food Insecurity Outlooks currently extends back only to mid-2011.

398 (ii) SADC CSC's issues probabilistic seasonal-scale rainfall forecasts. These forecasts are based  
399 on multiple models (both statistical and dynamical) as well as subjective expert assessments,  
400 which makes comparison with purely quantitative products inappropriate. Additionally, the  
401 archive of purely quantitative forecasts from SADC CSC only goes back to 2017.

402 Finally, the NHyFAS products are intended to be used as an addition to the existing early  
403 warning tools of FEWS NET and SADC CSC, which are partners in the efforts described in this  
404 study, rather than replacing any of the existing tools.

405

## 406 **4.2 Influence of crop yield on regional food insecurity and issues in crop yield reports**

407 In this study, it is assumed that when the SA region faces a production shortfall, the  
408 regional food insecurity is likely to rise. This was certainly the case during the 2015-16 El Niño,  
409 the most recent major food insecurity event in the region (SADC 2016). However, this  
410 assumption ignores other important factors that may lead to or further worsen food insecurity in  
411 the region, such as inadequate agricultural inputs, price shocks (which can be global in nature),  
412 rise in population, conflict, limited livelihood options, stocks, etc. Nonetheless, the direct  
413 relationship of crop yield with the interannual variability in available moisture makes RZSM an

414 important variable for food security monitoring and thus, it is of keen interest to early warning  
415 systems like FEWS NET, which is presently the primary end user of the NHyFAS. Crop yield  
416 early warning based on the NHyFAS products are also directly relevant to international  
417 collaborative efforts like the GEOGLAM initiative ([Becker-Reshef et al. 2018; Becker-Reshef et](#)  
418 [al. 2019](#)) and, particularly, to the Crop Monitor for Early Warning (<https://cropmonitor.org/>),  
419 which provides monthly assessments of crop conditions for the countries most vulnerable to food  
420 insecurity. Such assessments are key to reducing the uncertainty of crop prospects as the growing  
421 season progresses, and to providing critical evidence for informing food security decisions by  
422 humanitarian organizations and governments alike.

423 It is also worth noting that crop yield reports can be influenced by external factors (for  
424 example, reporting issues related to methods) other than long-term agricultural, technology-  
425 driven changes and climate interannual variability. The effect of these factors on the regional  
426 crop yield, of course, cannot be discounted by the detrending method employed in this study.

#### 427 **4.3 Reliance on single climate model forecasts:**

428 Finally, the results of this study are also likely affected by the use of only one dynamical  
429 climate forecast model for driving the seasonal hydrologic forecasting system. Adding forecasts  
430 from more climate and hydrologic models would likely enhance the skill of the system ([Kirtman](#)  
431 [et al. 2014; Krishnamurti et al. 1999](#)). The choice of one dynamical system was made mostly for  
432 logistical purposes, since GEOS archived and real-time forecasts include all atmospheric forcing  
433 variables needed to drive such LSMs, and are available through NASA-GSFC routinely, to  
434 facilitate operational production of NHyFAS forecasts.

435 **5 Conclusions**

436 The region of SA witnessed several severe food insecurity events in the last few decades.  
437 Mitigation of food insecurity impact requires timely and effective interventions by national,  
438 regional, and international agencies. To support those interventions, early warning of food  
439 insecurity is needed. In this study, we investigate the suitability of the operational RZSM  
440 products produced by a recently developed NASA seasonal scale hydrologic forecasting system,  
441 NHyFAS, in supporting food insecurity early warning in this region.

442 The key findings of this study are: (i) the NHyFAS products would have identified the  
443 regional severe 2015-2016 drought event (which peaked in December-February) at least as early  
444 as November 1st of 2015; (ii) February RZSM forecasts produced as early as November 1 (4-5  
445 months before the start of harvest, and about one year before the start of the next lean season)  
446 can explain the interannual variability in regional crop yield production with moderate skill  
447 (correlation 0.49); (iii) use of dynamical climate forecasts adds to the skill (relative to the skill  
448 coming from the initial hydrologic conditions alone) in predicting regional crop yield through the  
449 prediction of February RZSM; (iv) the February RZSM monitoring product, available in early  
450 March (1-2 months before the start of harvest and 8-9 months before the start of the next lean  
451 season) can explain the variability in regional crop yield with high skill (correlation of 0.79); (v)  
452 when the February RZSM forecast (initialized on November 1) is found to be in the lowest  
453 tercile, the subsequent detrended regional crop yield is below normal about 66% of the time  
454 (statistical significance level ~86%), and likewise, when the February RZSM monitoring product  
455 is in the lowest tercile, the subsequent crop yield is (for a limited set of samples considered)  
456 always below normal (statistical significance level >95%); (vi) the February RZSM monitoring  
457 product can provide “out-of-sample” crop yield forecasts with higher skill than DJF ENSO (38%

458 reduction in mean error relative to DJF ENSO), whereas the February RZSM forecasting  
459 product, available in early November, can provide crop yield forecasts with comparable skill  
460 (~6% increase in mean error relative to DJF ENSO).

461         The NHyFAS products described here were first generated in August 2018 for  
462 operational applications by FEWS NET. As described in much detail in Funk et al., (2019), each  
463 month, FEWS NET’s regional scientists (located in eastern, western, and southern Africa)  
464 review the latest products ahead of the FEWS NET’s monthly climate discussions. The NHyFAS  
465 products, in addition to other early warning tools, are used to support or revise the assumptions  
466 of climate and hydrologic conditions in the upcoming season. The updated assumptions are then  
467 passed on to food analysts for the region in order to help inform needed relief actions. This study  
468 demonstrates the value of the NHyFAS products in supporting food insecurity early warning in  
469 the SA region. It is worth mentioning that since NHyFAS currently covers Africa and the Middle  
470 East region, the NHyFAS products are applicable for food insecurity early warning in the rest of  
471 Africa and the Middle East as well. Based on this study, it is postulated (future research pending)  
472 that NHyFAS RZSM products can be particularly effective for those rainfed agriculture regions  
473 and seasons which are not known to have strong teleconnection (e.g. with ENSO), as in the SA  
474 region. Finally, since the data sets and models used to implement the NHyFAS are available  
475 globally, a similar seasonal RZSM monitoring and forecasting framework can be developed at a  
476 global scale to support food insecurity early warning in other rainfed regions across the globe.

477

478 **Author contribution:** SS led the design of the analysis, conducted the analysis, and wrote the  
479 manuscript and generated figures. KA, CPL, CF, and FD contributed to the design of the  
480 analysis. FD contributed to the analysis as well. KA and AH conducted the model simulations.  
481 RK and CPL reviewed the article and proposed substantial changes. CPL and GH are PIs of  
482 projects supporting this work. TM, JV, AM, AH facilitate real-time application of the products.  
483 The other co-authors reviewed the article and provided their input/edits.



484 **Competing interests:**

485 The authors declare that they have no conflict of interest.

486

487

488

489

490

491

492

493

494

495

496

497

498

499

500

501

502

503

504

505

506

507 **Acknowledgements:**

508 Support for this study comes from NASA Grant NNX15AL46G and the US Geological Survey  
509 (USGS) cooperative agreement #G09AC000001. Crop yield, production, and consumption data  
510 were obtained from USDA FAS's PSD:

511 <https://apps.fas.usda.gov/psdonline/app/index.html#/app/home>. Average price data were obtained

512 from FAO's FAO STATS database <http://www.fao.org/faostat/en/#home>. World Bank

513 Development Indicators were downloaded from <https://data.worldbank.org/indicator/>. GEOS

514 forecast data sets are generated and supported by NASA's Global Modeling and Assimilation

515 Office (GMAO). Model source code can be found at NASA's Land Information System's

516 GitHub repository (<https://lis.gsfc.nasa.gov/news/latest-lis-code-now-available-github>). Model

517 parameters are available through email request. The daily CHIRPS precipitation data can be

518 found here ([ftp://ftp.chg.ucsb.edu/pub/org/chg/products/CHIRPS-2.0/global\\_daily/netcdf/p25/](ftp://ftp.chg.ucsb.edu/pub/org/chg/products/CHIRPS-2.0/global_daily/netcdf/p25/)).

519 MERRA-2 reanalysis-based atmospheric forcings can be found through NASA's GES DISC

520 archive ([https://disc.gsfc.nasa.gov/datasets?keywords=%22MERRA-](https://disc.gsfc.nasa.gov/datasets?keywords=%22MERRA-2%22&page=1&source=Models%2FAnalyses%20MERRA-2)

521 [2%22&page=1&source=Models%2FAnalyses%20MERRA-2](https://disc.gsfc.nasa.gov/datasets?keywords=%22MERRA-2%22&page=1&source=Models%2FAnalyses%20MERRA-2)). NHyFAS forecasts, in the form

522 of maps, can be found here <https://lis.gsfc.nasa.gov/projects/nhyfas>. As of now, NHyFAS

523 forecast data sets are not publicly accessible. High-performance computing resources were

524 provided by the NASA Center for Climate Simulation (NCCS) in Greenbelt, MD. The authors

525 thank Climate Hazards Center's technical writer, Juliet Way-Henthorne, for providing

526 professional editing.

527

528

529

530

531

532  
533  
534  
535  
536

## References

- 537 Archer, E., Landman, W. A., Tadross, M. A., Malherbe, J., Weepener, H., Maluleke, P. and  
538 Marumbwa, F. M.: Understanding the evolution of the 2014–2016 summer rainfall seasons in  
539 southern Africa: Key lessons, *Climate Risk Management*, 16, 22–28, 2017.
- 540 Arsenault, K., Shukla, S., Hazra, A., Getirana, A., McNally, A., Kumar, S., Koster, R., Zaitchik,  
541 B., Badr, H., Jung, H. C., Narapusetty, B., Navari, M., Wang, S., Mocko, S., Funk, C., Harrison,  
542 L., Husak, G., Verdin, J. V., and Peters-Lidard, C. C.: A NASA modeling and remote-sensing  
543 based hydrological forecast system for food and water security applications. *Bulletin of the*  
544 *American Meteorological Society (in review)*
- 545 Borovikov, A., Cullather, R., Kovach, R., Marshak, J., Vernieres, G., Vikhliayev, Y., Zhao, B. and  
546 Li, Z.: GEOS-5 seasonal forecast system, *Clim. Dyn.*, doi:10.1007/s00382-017-3835-2, 2017.
- 547 Cane, M. A., Eshel, G. and Buckland, R. W.: Forecasting Zimbabwean maize yield using eastern  
548 equatorial Pacific sea surface temperature, *Nature*, 370(6486), 204–205, 1994.
- 549 Csiszar, I. and Gutman, G.: Mapping global land surface albedo from NOAA AVHRR, *Journal*  
550 *of Geophysical Research: Atmospheres*, 104(D6), 6215–6228, doi:10.1029/1998jd200090, 1999.
- 551 Davenport, F. M., Harrison, L., Shukla, S., Husak, G., Funk, C. and McNally, A.: Using out-of-  
552 sample yield forecast experiments to evaluate which earth observation products best indicate end  
553 of season maize yields, *Environmental Research Letters*, 14(12), 124095, doi:10.1088/1748-  
554 9326/ab5ccd, 2019.
- 555 Diro, G. T.: Skill and economic benefits of dynamical downscaling of ECMWF ENSEMBLE  
556 seasonal forecast over southern Africa with RegCM4, *Int. J. Climatol.*, 36(2), 675–688, 2015.
- 557 Ducharne, A., Koster, R. D., Suarez, M. J., Stieglitz, M. and Kumar, P.: A catchment-based  
558 approach to modeling land surface processes in a general circulation model: 2. Parameter  
559 estimation and model demonstration, *J. Geophys. Res. D: Atmos.*, 105(D20), 24823–24838,  
560 2000.
- 561 Friedl, M. A., McIver, D. K., Hodges, J. C. F., Zhang, X. Y., Muchoney, D., Strahler, A. H.,  
562 Woodcock, C. E., Gopal, S., Schneider, A., Cooper, A., Baccini, A., Gao, F. and Schaaf, C.:  
563 Global land cover mapping from MODIS: algorithms and early results, *Remote Sensing of*  
564 *Environment*, 83(1-2), 287–302, doi:10.1016/s0034-4257(02)00078-0, 2002.
- 565 Funk, C., Peterson, P., Landsfeld, M., Pedreros, D., Verdin, J., Shukla, S., Husak, G., Rowland,  
566 J., Harrison, L., Hoell, A. and Michaelsen, J.: The climate hazards infrared precipitation with  
567 stations--a new environmental record for monitoring extremes, *Sci Data*, 2, 150066, 2015.
- 568 Funk, C., Davenport, F., Harrison, L., Magadzire, T., Galu, G., Artan, G. A., Shukla, S.,  
569 Korecha, D., Indeje, M., Pomposi, C., Macharia, D., Husak, G. and Nsadisa, F. D.:

570 Anthropogenic Enhancement of Moderate-to-Strong El Niño Events Likely Contributed to  
571 Drought and Poor Harvests in Southern Africa During 2016, *Bull. Am. Meteorol. Soc.*, 99(1),  
572 S91–S96, 2018.

573 Funk, C., Shukla, S., Thiaw, W. M., Rowland, J., Hoell, A., McNally, A., Husak, G., Novella,  
574 N., Budde, M., Peters-Lidard, C., Adoum, A., Galu, G., Korecha, D., Magadzire, T., Rodriguez,  
575 M., Robjhon, M., Bekele, E., Arsenault, K., Peterson, P., Harrison, L., Fuhrman, S., Davenport,  
576 F., Landsfeld, M., Pedreros, D., Jacob, J. P., Reynolds, C., Becker-Reshef, I. and Verdin, J.:  
577 Recognizing the Famine Early Warning Systems Network (FEWS NET): Over 30 Years of  
578 Drought Early Warning Science Advances and Partnerships Promoting Global Food Security,  
579 *Bulletin of the American Meteorological Society*, doi:10.1175/bams-d-17-0233.1, 2019.

580 Gelaro, R., McCarty, W., Suárez, M. J., Todling, R., Molod, A., Takacs, L., Randles, C. A.,  
581 Darmenov, A., Bosilovich, M. G., Reichle, R., Wargan, K., Coy, L., Cullather, R., Draper, C.,  
582 Akella, S., Buchard, V., Conaty, A., Da Silva, A. M., Gu, W., Kim, G., Koster, R., Lucchesi, R.,  
583 Merkova, D., Nielsen, J. E., Partyka, G., Pawson, S., Putman, W., Rienecker, M., Schubert, S.  
584 D., Sienkiewicz, M. and Zhao, A. B.: The Modern-Era Retrospective Analysis for Research and  
585 Applications, Version 2 (MERRA-2), *J. Climate*, 30, 5419–5454, 2017.

586 Guo, Z. and Dirmeyer, P. A.: Evaluation of the Second Global Soil Wetness Project soil moisture  
587 simulations: 1. Intermodel comparison, *Journal of Geophysical Research*, 111(D22),  
588 doi:10.1029/2006jd007233, 2006.

589 Gutman, G. and Ignatov, A.: The derivation of the green vegetation fraction from  
590 NOAA/AVHRR data for use in numerical weather prediction models, *International Journal of*  
591 *Remote Sensing*, 19(8), 1533–1543, doi:10.1080/014311698215333, 1998.

592 Hoell, A. and Cheng, L.: Austral summer Southern Africa precipitation extremes forced by the  
593 El Niño–Southern oscillation and the subtropical Indian Ocean dipole, *Clim. Dyn.*, 50(9-10),  
594 3219–3236, 2017.

595 Hoell, A., Funk, C., Zinke, J. and Harrison, L.: Modulation of the Southern Africa precipitation  
596 response to the El Niño Southern Oscillation by the subtropical Indian Ocean Dipole, *Clim.*  
597 *Dyn.*, 48(7-8), 2529–2540, 2016.

598 Hoell, A., Gaughan, A. E., Shukla, S. and Magadzire, T.: The Hydrologic Effects of  
599 Synchronous El Niño–Southern Oscillation and Subtropical Indian Ocean Dipole Events over  
600 Southern Africa, *J. Hydrometeorol.*, 18(9), 2407–2424, 2017.

601 Hyndman, R. J. and Athanasopoulos, G.: *Forecasting: principles and practice*, OTexts., 2018.

602 Hyndman, R. J. and Khandakar, Y.: *Automatic Time Series for Forecasting: The Forecast*  
603 *Package for R*, 2007.

604 Koster, R. D., Suarez, M. J., Ducharme, A., Stieglitz, M. and Kumar, P.: A catchment-based  
605 approach to modeling land surface processes in a general circulation model: 1. Model structure,  
606 *J. Geophys. Res. D: Atmos.*, 105(D20), 24809–24822, 2000.

607 Kumar, S., Peterslidard, C., Tian, Y., Houser, P., Geiger, J., Olden, S., Lighty, L., Eastman, J.,

608 Doty, B. and Dirmeyer, P.: Land information system: An interoperable framework for high  
609 resolution land surface modeling, *Environmental Modelling & Software*, 21(10), 1402–1415,  
610 2006.

611 Landman, W. A. and Beraki, A.: Multi-model forecast skill for mid-summer rainfall over  
612 southern Africa, *Int. J. Climatol.*, 32(2), 303–314, 2010.

613 Landman, W. A. and Goddard, L.: Statistical Recalibration of GCM Forecasts over Southern  
614 Africa Using Model Output Statistics, *J. Clim.*, 15(15), 2038–2055, 2002.

615 Landman, W. A., Mason, S. J., Tyson, P. D. and Tennant, W. J.: Retro-active skill of multi-tiered  
616 forecasts of summer rainfall over southern Africa, *Int. J. Climatol.*, 21(1), 1–19, 2001.

617 Manatsa, D., Mushore, T. and Lenouo, A.: Improved predictability of droughts over southern  
618 Africa using the standardized precipitation evapotranspiration index and ENSO, *Theor. Appl.*  
619 *Climatol.*, 127(1-2), 259–274, 2015.

620 Martin, R. V., Washington, R. and Downing, T. E.: Seasonal Maize Forecasting for South Africa  
621 and Zimbabwe Derived from an Agroclimatological Model, *J. Appl. Meteorol.*, 39(9), 1473–  
622 1479, 2000.

623 Meque, A. and Abiodun, B. J.: Simulating the link between ENSO and summer drought in  
624 Southern Africa using regional climate models, *Clim. Dyn.*, 44(7-8), 1881–1900, 2014.

625 Moody, E. G., King, M. D., Schaaf, C. B. and Platnick, S.: MODIS-Derived Spatially Complete  
626 Surface Albedo Products: Spatial and Temporal Pixel Distribution and Zonal Averages, *Journal*  
627 *of Applied Meteorology and Climatology*, 47(11), 2879–2894, doi:10.1175/2008jamc1795.1,  
628 2008.

629 Niu, G.-Y., Yang, Z.-L., Mitchell, K. E., Chen, F., Ek, M. B., Barlage, M., Kumar, A., Manning,  
630 K., Niyogi, D., Rosero, E., Tewari, M. and Xia, Y.: The community Noah land surface model  
631 with multiparameterization options (Noah-MP): 1. Model description and evaluation with local-  
632 scale measurements, *J. Geophys. Res.*, 116(D12), doi:10.1029/2010jd015139, 2011.

633 Pomposi, C., Funk, C., Shukla, S., Harrison, L. and Magadzire, T.: Distinguishing southern  
634 Africa precipitation response by strength of El Niño events and implications for decision-  
635 making, *Environ. Res. Lett.*, 13(7), 074015, 2018.

636 Reynolds, C. A., Jackson, T. J. and Rawls, W. J.: Estimating soil water-holding capacities by  
637 linking the Food and Agriculture Organization Soil map of the world with global pedon  
638 databases and continuous pedotransfer functions, *Water Resources Research*, 36(12), 3653–  
639 3662, doi:10.1029/2000wr900130, 2000.

640 SADC: SADC Regional Vulnerability Assessment and Analysis Synthesis Report 2016: State of  
641 Food Insecurity and Vulnerability in the Southern African Development Community : Compiled  
642 from the National Vulnerability Assessment Committee (NVAC) Reports Presented at the  
643 Regional Vulnerability Assessment and Analysis (RVAA) Annual Dissemination Forum on 6-10  
644 June 2016 in Pretoria, Republic of South Africa., 2016.

645 Sheffield, J., Wood, E. F., Chaney, N., Guan, K., Sadri, S., Yuan, X., Olang, L., Amani, A., Ali,  
646 A., Demuth, S. and Ogallo, L.: A Drought Monitoring and Forecasting System for Sub-Sahara  
647 African Water Resources and Food Security, *Bull. Am. Meteorol. Soc.*, 95(6), 861–882, 2014.

648 Shukla, S., McNally, A., Husak, G. and Funk, C.: A seasonal agricultural drought forecast  
649 system for food-insecure regions of East Africa, *Hydrology and Earth System Sciences*  
650 *Discussions*, 11(3), 3049–3081, doi:10.5194/hessd-11-3049-2014, 2014.

651 Sunday, R. K. M., Masih, I., Werner, M. and van der Zaag, P.: Streamflow forecasting for  
652 operational water management in the Incomati River Basin, Southern Africa, *Physics and*  
653 *Chemistry of the Earth, Parts A/B/C*, 72-75, 1–12, 2014.

654 Tamuka Magadzire, G. G. A. J. P. V.: How climate forecasts strengthen food security, WMO.  
655 [online] Available from: [https://public.wmo.int/en/resources/bulletin/how-climate-forecasts-](https://public.wmo.int/en/resources/bulletin/how-climate-forecasts-strengthen-food-security)  
656 [strengthen-food-security](https://public.wmo.int/en/resources/bulletin/how-climate-forecasts-strengthen-food-security) (Accessed 23 January 2020), 2017.

657 Trambauer, P., Werner, M., Winsemius, H. C., Maskey, S., Dutra, E. and Uhlenbrook, S.:  
658 Hydrological drought forecasting and skill assessment for the Limpopo River basin, southern  
659 Africa, *Hydrol. Earth Syst. Sci.*, 19(4), 1695–1711, 2015.

660 Verdin, K. L. and Verdin, J. P.: A topological system for delineation and codification of the  
661 Earth’s river basins, *Journal of Hydrology*, 218(1-2), 1–12, doi:10.1016/s0022-1694(99)00011-6,  
662 1999.

663 Winsemius, H. C., Dutra, E., Engelbrecht, F. A., Van Garderen, E. A., Wetterhall, F.,  
664 Pappenberger, F. and Werner, M. G. F.: The potential value of seasonal forecasts in a changing  
665 climate in southern Africa, *Hydrol. Earth Syst. Sci.*, 18(4), 1525–1538, 2014.

666 Wood, A. W., Maurer, E. P. and Kumar, A., and Lettenmaier, D. P: Long-range experimental  
667 hydrologic forecasting for the eastern United States, *J. Geophys. Res.*, 107(D20),  
668 doi:10.1029/2001jd000659, 2002.

669 Yang, Z.-L., Niu, G.-Y., Mitchell, K. E., Chen, F., Ek, M. B., Barlage, M., Longuevergne, L.,  
670 Manning, K., Niyogi, D., Tewari, M. and Xia, Y.: The community Noah land surface model with  
671 multiparameterization options (Noah-MP): 2. Evaluation over global river basins, *J. Geophys.*  
672 *Res.*, 116(D12), doi:10.1029/2010jd015140, 2011.

673 Yuan, X., Wood, E. F., Chaney, N. W., Sheffield, J., Kam, J., Liang, M. and Guan, K.:  
674 Probabilistic Seasonal Forecasting of African Drought by Dynamical Models, *Journal of*  
675 *Hydrometeorology*, 14(6), 1706–1720, doi:10.1175/jhm-d-13-054.1, 2013.

676 Yuan, X., Wang, L. and Wood, E. F.: Anthropogenic Intensification of Southern African Flash  
677 Droughts as Exemplified by the 2015/16 Season, *Bulletin of the American Meteorological*  
678 *Society*, 99(1), S86–S90, doi:10.1175/bams-d-17-0077.1, 2018.

679 Niu, G.-Y., Yang, Z.-L., Mitchell, K. E., Chen, F., Ek, M. B., Barlage, M., Kumar, A., Manning,  
680 K., Niyogi, D., Rosero, E., Tewari, M. and Xia, Y.: The community Noah land surface model  
681 with multiparameterization options (Noah-MP): 1. Model description and evaluation with local-  
682 scale measurements, *J. Geophys. Res.*, 116(D12), doi:10.1029/2010jd015139, 2011.

683 Pomposi, C., Funk, C., Shukla, S., Harrison, L. and Magadzire, T.: Distinguishing southern  
684 Africa precipitation response by strength of El Niño events and implications for decision-  
685 making, *Environ. Res. Lett.*, 13(7), 074015, 2018.

686 SADC: SADC Regional Vulnerability Assessment and Analysis Synthesis Report 2016: State of  
687 Food Insecurity and Vulnerability in the Southern African Development Community : Compiled  
688 from the National Vulnerability Assessment Committee (NVAC) Reports Presented at the  
689 Regional Vulnerability Assessment and Analysis (RVAA) Annual Dissemination Forum on 6-10  
690 June 2016 in Pretoria, Republic of South Africa., 2016.

691 Sheffield, J., Wood, E. F., Chaney, N., Guan, K., Sadri, S., Yuan, X., Olang, L., Amani, A., Ali,  
692 A., Demuth, S. and Ogallo, L.: A Drought Monitoring and Forecasting System for Sub-Sahara  
693 African Water Resources and Food Security, *Bull. Am. Meteorol. Soc.*, 95(6), 861–882, 2014.

694 Shukla, S., McNally, A., Husak, G. and Funk, C.: A seasonal agricultural drought forecast  
695 system for food-insecure regions of East Africa, *Hydrology and Earth System Sciences*  
696 *Discussions*, 11(3), 3049–3081, doi:10.5194/hessd-11-3049-2014, 2014.

697 Sunday, R. K. M., Masih, I., Werner, M. and van der Zaag, P.: Streamflow forecasting for  
698 operational water management in the Incomati River Basin, Southern Africa, *Physics and*  
699 *Chemistry of the Earth, Parts A/B/C*, 72-75, 1–12, 2014.

700 Trambauer, P., Werner, M., Winsemius, H. C., Maskey, S., Dutra, E. and Uhlenbrook, S.:  
701 Hydrological drought forecasting and skill assessment for the Limpopo River basin, southern  
702 Africa, *Hydrol. Earth Syst. Sci.*, 19(4), 1695–1711, 2015.

703 Verdin, K. L. and Verdin, J. P.: A topological system for delineation and codification of the  
704 Earth’s river basins, *Journal of Hydrology*, 218(1-2), 1–12, doi:10.1016/s0022-1694(99)00011-6,  
705 1999.

706 Winsemius, H. C., Dutra, E., Engelbrecht, F. A., Van Garderen, E. A., Wetterhall, F.,  
707 Pappenberger, F. and Werner, M. G. F.: The potential value of seasonal forecasts in a changing  
708 climate in southern Africa, *Hydrol. Earth Syst. Sci.*, 18(4), 1525–1538, 2014.

709 Wood, A. W., Maurer, E. P. and Kumar, A., and Lettenmaier, D. P: Long-range experimental  
710 hydrologic forecasting for the eastern United States, *J. Geophys. Res.*, 107(D20),  
711 doi:10.1029/2001jd000659, 2002.

712 Yang, Z.-L., Niu, G.-Y., Mitchell, K. E., Chen, F., Ek, M. B., Barlage, M., Longuevergne, L.,  
713 Manning, K., Niyogi, D., Tewari, M. and Xia, Y.: The community Noah land surface model with  
714 multiparameterization options (Noah-MP): 2. Evaluation over global river basins, *J. Geophys.*  
715 *Res.*, 116(D12), doi:10.1029/2010jd015140, 2011.



716

717 Table 1: Performance of ‘out-of-sample’ crop yield forecasting over the validation period of

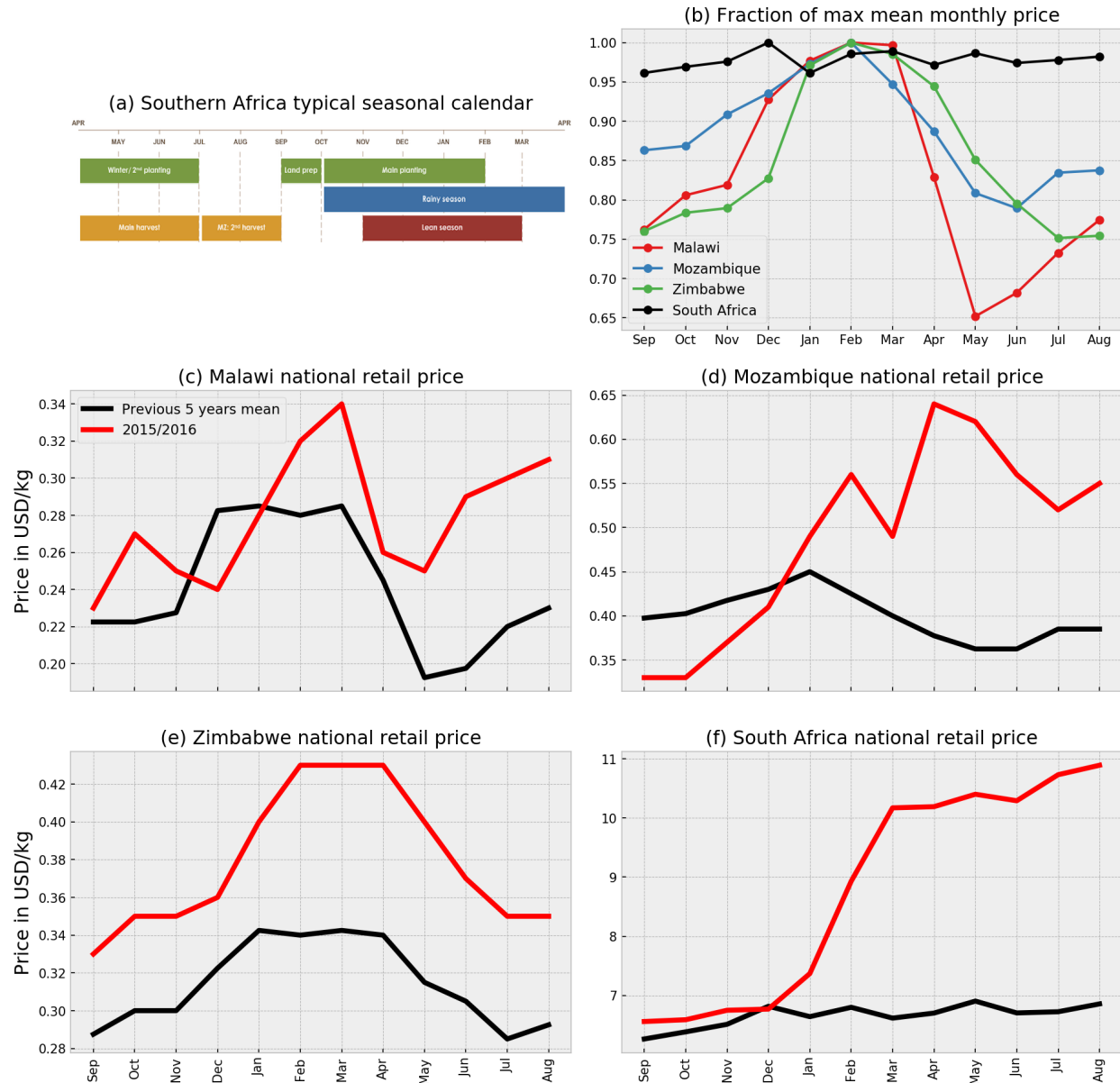
718 2008-2018.

719

	<b>Univariate model</b>	<b>Univariate model + ENSO</b>	<b>Univariate model + Feb-RZSM (Monitoring)</b>	<b>Univariate model + Feb-RZSM (forecast)</b>
<b>Mean absolute error over the validation period (MT/HA)</b>	0.342	0.285	0.174	0.301
<b>Number of years observed yield is within 95% confidence interval bound</b>	9	10	10	9
<b>Mean spread of 95% confidence interval (MT/HA)</b>	1.64	1.20	1.07	1.20
<b>Number of years observed yield is within 80% confidence interval bound</b>	9	7	10	7
<b>Mean spread of 80% confidence interval (MT/HA)</b>	1.07	0.78	0.70	0.78

720

721



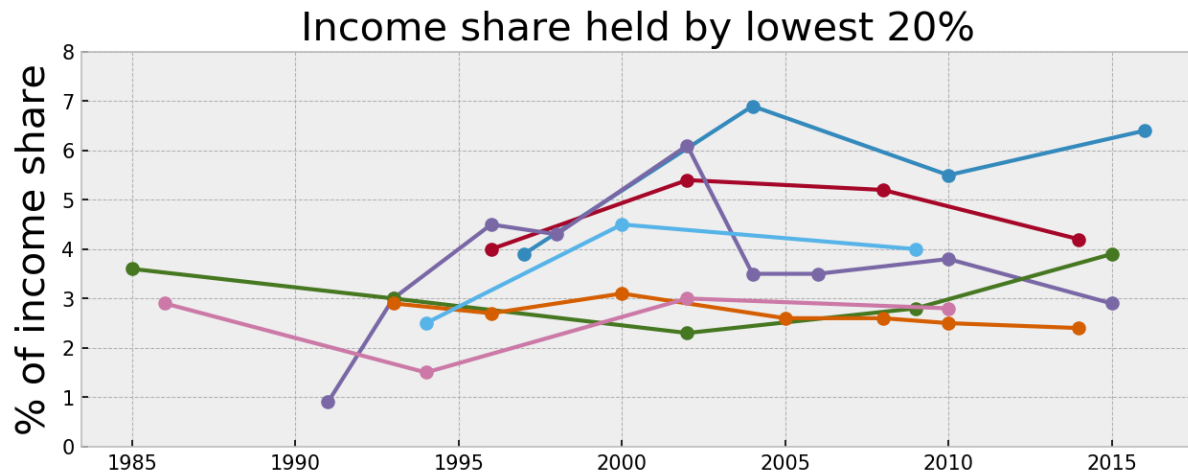
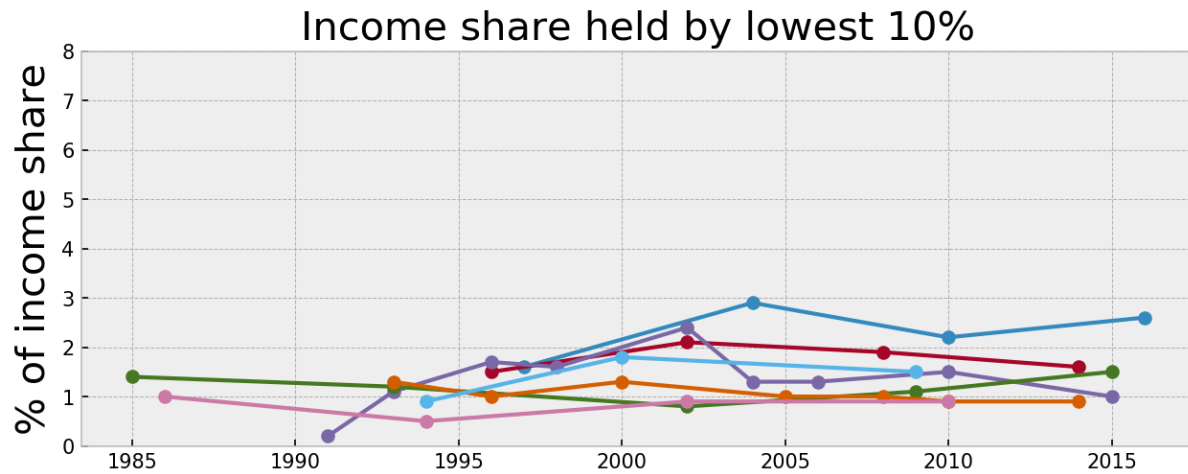
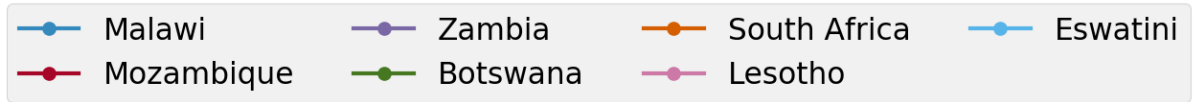
722

723

724 **Figure 1: (a) Schematic representation of a typical seasonal calendar for the southern**  
 725 **Africa region. (taken from: <http://fews.net/southern-africa>) (b) Monthly climatology of**  
 726 **maize prices in SA countries. The monthly mean prices are normalized relative to the**  
 727 **maximum mean monthly price for a given country, as the actual values of the mean**  
 728 **monthly prices are different for different countries. Comparison of mean monthly maize**

729 **prices for (c) Malawi (d) Mozambique (e) Zimbabwe (f) South Africa, during the 2015-16**  
730 **event (red line) with the previous 5-year mean prices (black line). The price data is**  
731 **available from FAOSTAT (FAO 2019).**

732

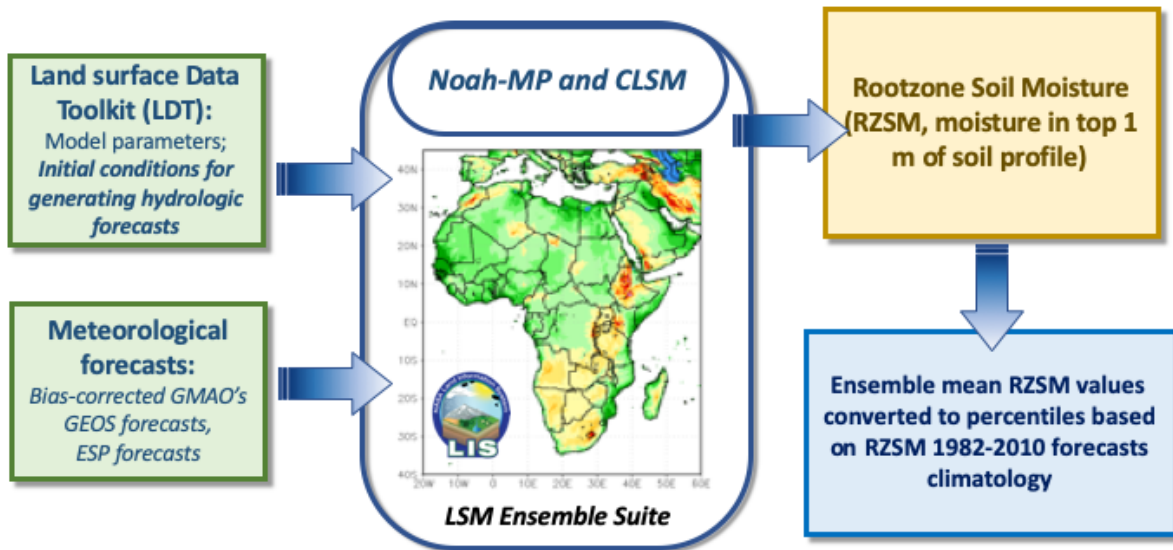


733

734

735 **Figure 2: Percentage of income share held by lowest 10% and 20% income population in**  
 736 **the Southern Africa countries. (Data Source: the World Bank's World Development**  
 737 **Indicators)**

738

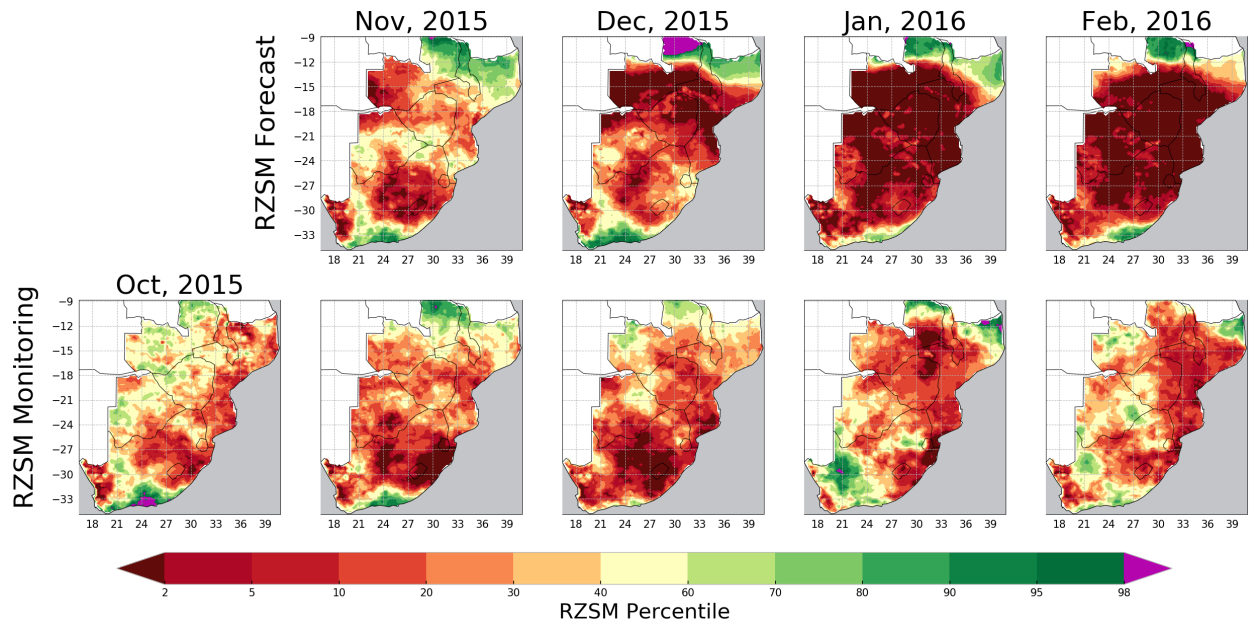


739

740 **Figure 3: Overview of the NHyFAS implementation to produce RZSM monitoring and**  
 741 **forecasting products, as used in this study.**

742

743



745

746

747

748

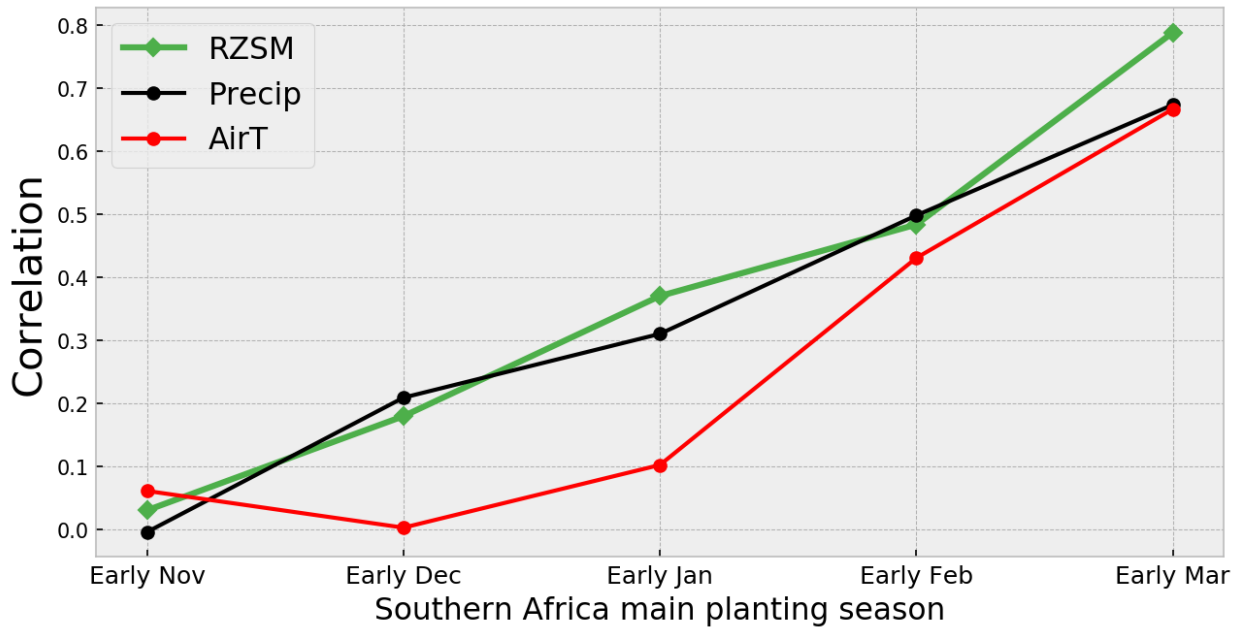
749

750

751

752

**Figure 4: Forecast (top panel) and Monitoring of Rootzone soil moisture (RZSM) percentiles for the months of November 2015 through February 2016. October 2015 conditions reflect the state of RZSM during the month preceding the forecast initialization on November 1, 2015. The RZSM monitoring product for a given month is available during the early part of the following month. The historical climatology (1982-2010) was used to calculate percentile.**



753

754

755

756

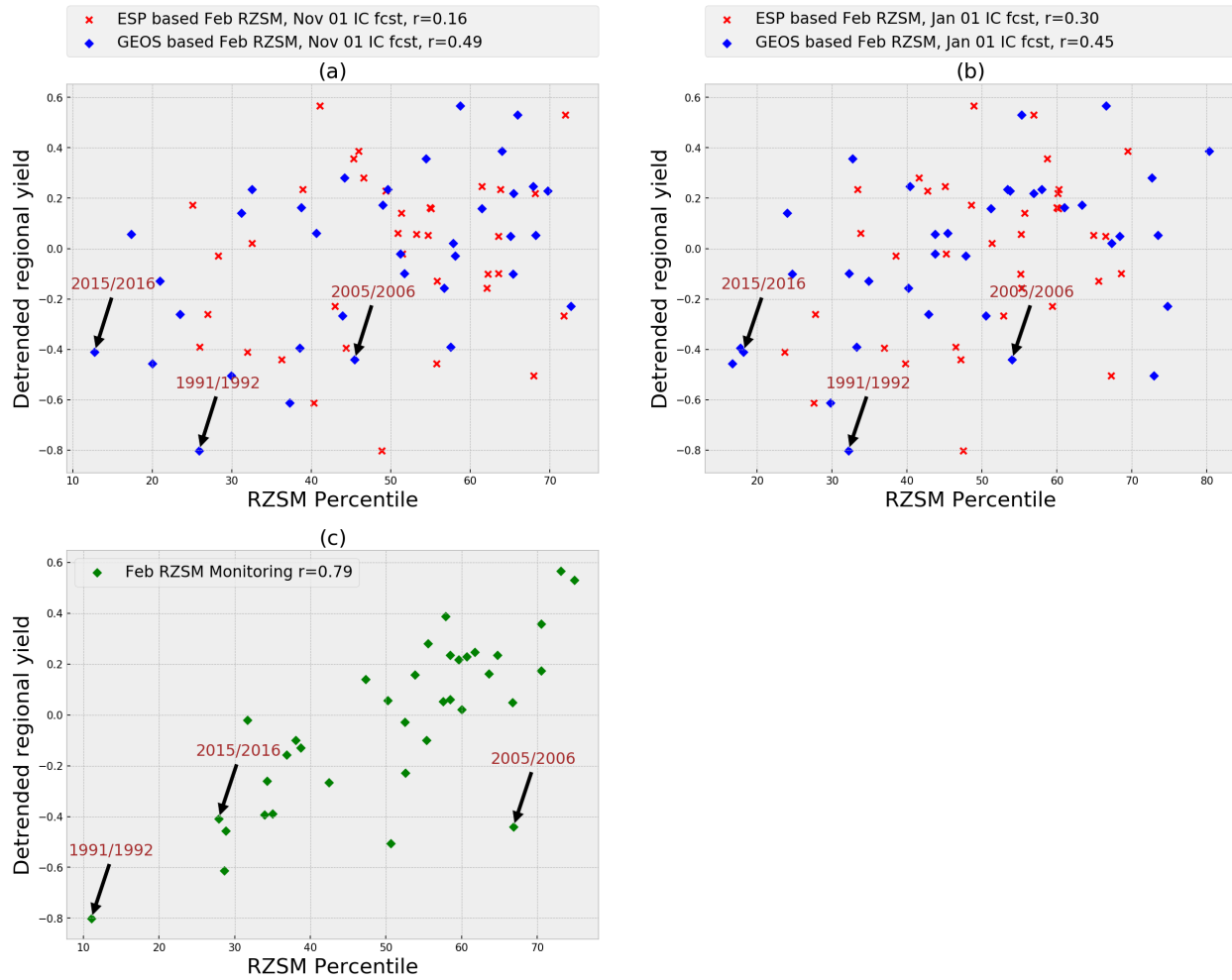
757

758

759

760

**Figure 5: Variability of the correlation between the 3-month seasonal precipitation, 3-month seasonal air temperature (AirT), and monthly RZSM monitoring product with the detrended crop yield. This result highlights that RZSM is potentially a better predictor of crop yield than seasonal precipitation and AirT; also, the skill is the highest in early March when DJF seasonal precipitation, AirT, and February RZSM monitoring products are available.**



761

762 **Figure 6: Covariability of detrended regional yield in southern Africa with: (a) February**

763 **RZSM forecasts (initialized on November 1) generated using ESP method and bias-**

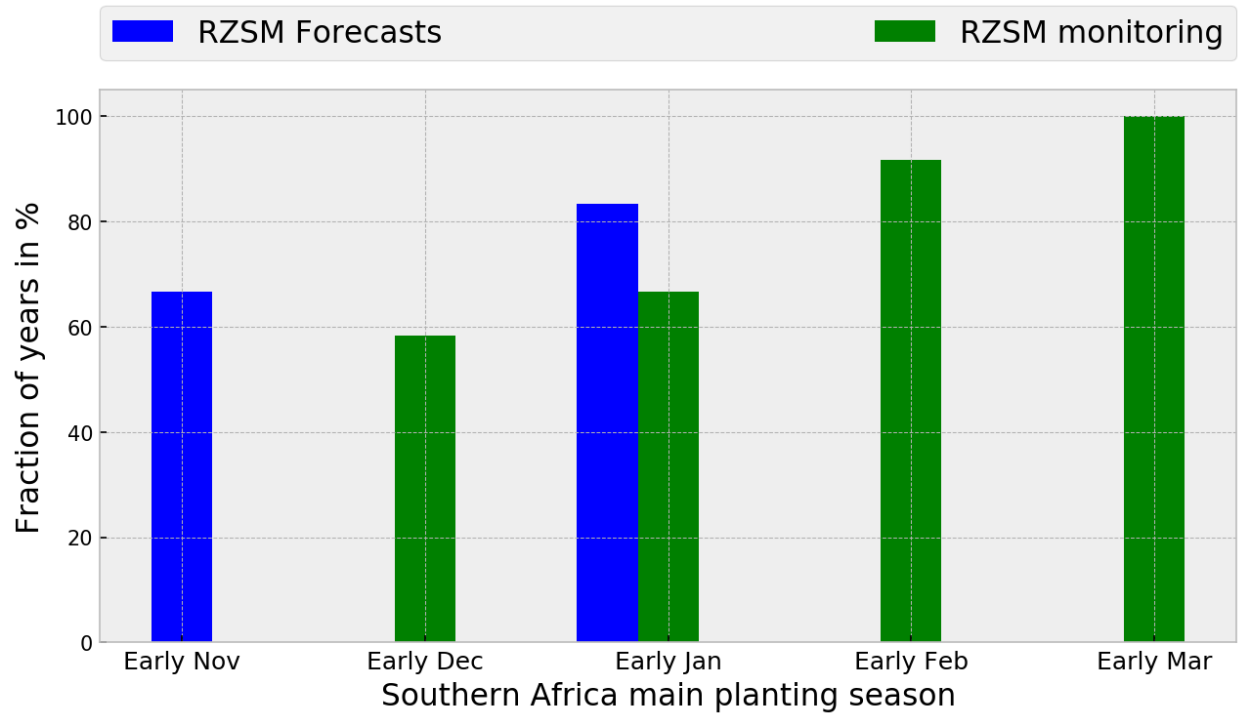
764 **corrected GEOS forecasts, (b) February RZSM forecasts (initialized on January 1)**

765 **generated using ESP method and bias-corrected GEOS forecasts, and (c) the February**

766 **RZSM monitoring product (available in early March).**

767

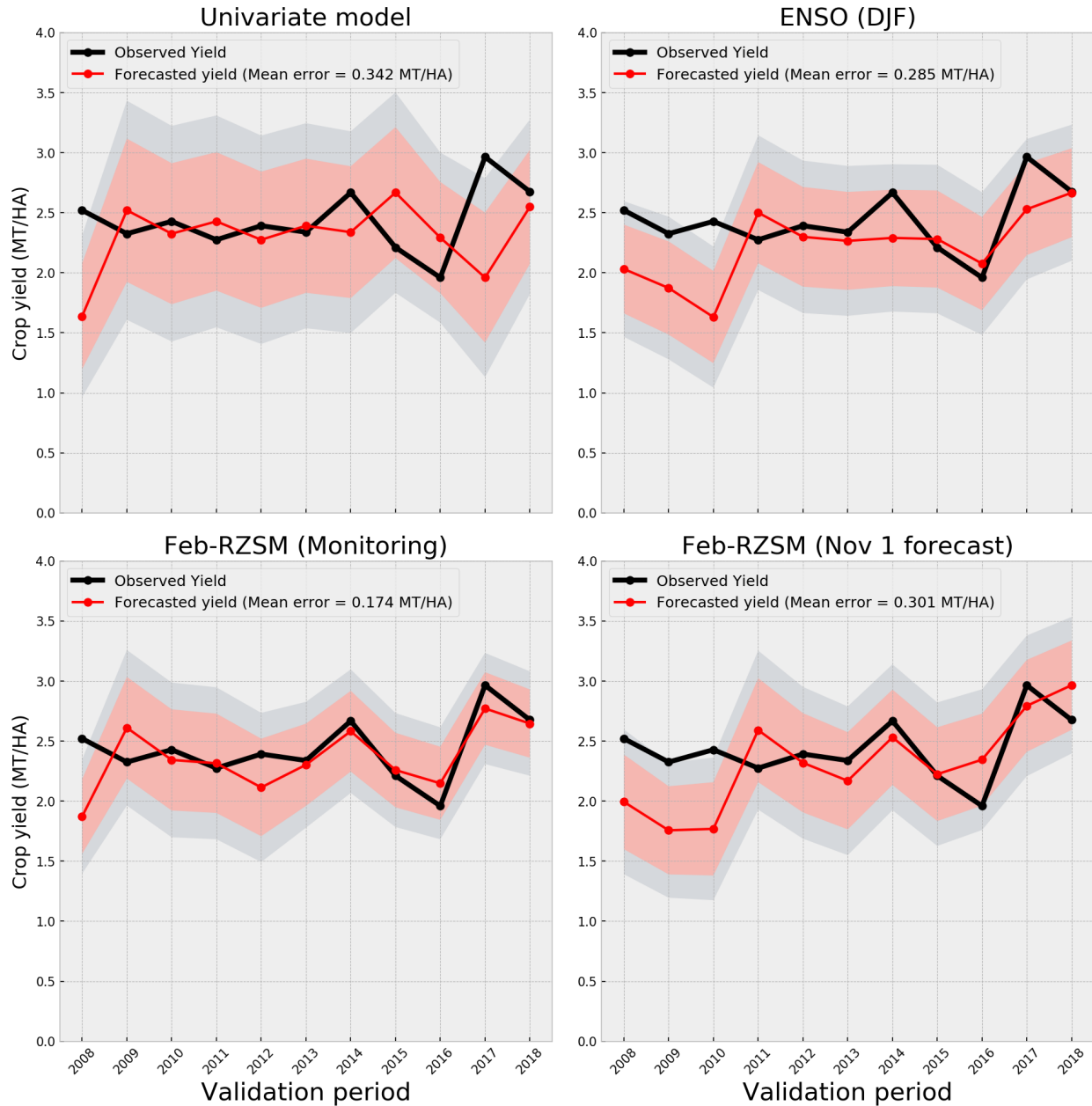




768

769

770 **Figure 7: Fraction of years with below-normal regional crop yield (based on the rank of**  
 771 **detrended crop yield) given that the corresponding RZSM forecasts (initialized on**  
 772 **November 1 and January 1) and RZSM monitoring product (available in early March)**  
 773 **were in the lowest tercile (based on the rank of the RZSM climatology). Note that the Nov 1**  
 774 **[Jan 1] RZSM forecasts-based probability of ~66% [~83%] is statistically significant at the**  
 775 **~86% [~95%] confidence level.**



776

777 **Figure 8: Comparison of the performance of a Univariate model alone, ENSO (DJF), Feb-**

778 **RZSM monitoring product, Feb-RZSM forecasting product as a predictor in forecasting**

779 **crop yield of Southern Africa. Pink [gray] shading indicates 80% [95%] confidence**

780 **interval.**